The International Journal of Advanced Manufacturing Technology (2023) 128:209–220
https://doi.org/10.1007/s00170-023-11751-0

ORIGINAL ARTICLE

Antibacterial evaluation of electroless Ni–P coating with ZnO nanoparticles on 3D printed ABS

Sebastián Restrepo[1,2] · María P. Duque[1] · Sindy Bello[3] · Laura M. Tirado[4] · Félix Echeverría[1] · Alejandro A. Zuleta[4] · Juan G. Castaño[1] · Esteban Correa[3]

Received: 22 February 2023 / Accepted: 7 June 2023 / Published online: 6 July 2023

Abstract
Acrylonitrile butadiene styrene (ABS) is one of the most widely used polymers in the manufacture of different parts in engineering applications. This polymer is sometimes subjected to metallizing processes that seek to modify the surface properties of the accessories. These processes often require the use of chromium and palladium. Some of the accessories in which ABS is used are subjected during their day-to-day use to environments in which they are prone to colonization of bacteria, generating multiple problems that affect both human health and the useful life of different equipment and devices. Recently, there have been great developments of nanoparticles with antibacterial properties, such as zinc oxides. However, these nanoparticles have not yet been incorporated and evaluated in metal coatings on ABS substrates with a view to conferring such properties on the polymer. This work implements the use of an electroless antibacterial Ni-P coating, modified with zinc oxide nanoparticles through processes free of chromium and palladium, on ABS substrates. The results showed that the addition of zinc oxide nanoparticles in quantities of 0.5 g/L and above in the electroless bath confer antibacterial characteristics on the surface for *S. aureus* under JIS Z 2801 standard. Through the methodology developed, the future development of 3D printed parts with metallized coating is possible, implementing processes chrome and palladium free, expanding the applications and uses of these.

Keywords Electroless nickel coatings · ZnO_2 nanoparticles · ABS

1 Introduction

Acrylonitrile butadiene styrene (ABS) is one of the most widely used thermoplastic polymers today, due to its interesting properties such as toughness, processability, corrosion resistance and low cost. This combination of properties is unmatched by any other thermoplastic material [1]. It is estimated that ABS consumption represents around 40% of total engineering plastic consumption worldwide [2]. Thanks to its excellent performance, its use in additive manufacturing techniques (3D printing) has become popular as it allows the manufacture of parts with high geometric complexity, maintaining and taking advantage of the properties of the material, all at a low cost [3]. Given its frequent use in 3D printing, it has generated interest in improved surface properties of ABS-printed parts. This could expand the range of applications, allowing these parts to be used in other environments previously unavailable, without the need to resort to more complex additive manufacturing techniques. An alternative to achieve this are metallization processes, which have the purpose of conferring properties on the parts such as resistance to abrasion, corrosion, electrical conductivity, reflectivity and aesthetic properties [1], this would make it possible to use these parts in applications such as automotive components, cosmetic packaging, computers, toys, cell phones, clocks, watches and various plastic appliances [4]

✉ Sebastián Restrepo
restrepovelez.sebastian@gmail.com

1 Centro de Investigación, Innovación y Desarrollo de Materiales – CIDEMAT, Universidad de Antioquia, Medellín, Colombia

2 Grupo de Investigación Industrial en Diseño de Materiales a partir de Minerales y Procesos – IDIMAP, Sumicol S.A.S, Sabaneta, Colombia

3 Materiales con Impacto – MAT&MPAC, Universidad de Medellín, Medellín, Colombia

4 Grupo de Investigación de Estudios en Diseño - GED, Facultad de Diseño Industrial, Universidad Pontificia Bolivariana, Circular 1 No 70-01, Medellín, Colombia

such as taps, door locks, cars and toilet flush buttons. An alternative to modify the surface properties are metallized coating processes.

Due to the nature of their applications, these parts are constantly subjected to contact with different users and, in some cases, to environments with high biological pollution, which make them susceptible to the formation and proliferation of colonies of bacteria on their surface, generating an important source of disease spread [5]. The colonization of surfaces and bacterial proliferation is a serious and growing concern in daily life, not only for human health but also for different industries such as paints, textiles, ceramic coatings, water treatment, marine transport, medicine, and food packaging [6]. Surface bacteria are housed in biofilms, which consist of microbial aggregates that adhere to the surface and generate 80% of microbial infections. These are responsible for more than 16 million cases of death by pathology per year in the USA [7].

Due to this problem, the development of antibacterial coatings has been explored from different approaches, employing electrochemical processes (such as galvanoplasty), chemical vapor deposition, powder metallurgy of thermal plasma, and sol-gel and cold spraying processes [8]. Many of these methods allow the development of antibacterial surfaces on different substrates, but they still present great technical and economic limitations that do not allow their use in parts manufactured by additive manufacturing.

In recent years, electroless coating processes have emerged as a useful metallization method and as an alternative to chrome plating processes. They have attracted great technological interest since no expensive equipment is needed [1], and enable the formation of homogeneous coatings on objects with complex geometries, providing excellent chemical and corrosion resistance, high hardness, good surface appearance, weldability and a good metal deposit rate [9]. Some electroless coatings have attracted significant interest within an industrial context, such as nickel alloys-phosphorus (Ni-P) and nickel-boron (Ni-B) which represents around 95% of industrial electroless coating applications [10]. Specifically, Ni-P alloys have been commercially successful due to their low-cost comparative to other electroless coatings (e.g., electroless Ni-B) and provide versatility in the process conserving surface properties compared to other electrolytic coatings [11].

However, although electroless Ni-P coatings provide satisfactory performance for several applications, improving their ability to adapt to different end uses justifies further development of them [12]. For example, nanoparticles of different natures are often incorporated into coatings in order to enhance their surface properties such as hardness, corrosion and wear resistance [13]. Due to this, a diversity of nanoparticles such as SiO_2 [14], Al_2O_3 [15], SiC [16], TiO_2 [13], and Fe_3O_4 [17] have been co-deposited. An example of this is the hardness of the coating, which some authors modified by incorporating different particles such as silicon nitride, cerium oxide and titanium oxide. The incorporation of these hard particles increased the hardness around 200, 150 and 120 hardness points, respectively, compared to Ni-P coatings without particles [18].

It is well known that some nanoparticles possess antibacterial behavior due to their chemical and physical characteristics that allow the interaction with microorganisms through various mechanisms, mitigating their growth and proliferation by damaging the cell wall of the bacteria, which inhibits its entry into the human body and its subsequent propagation [19–21]. Silver and copper metallic nanoparticles, graphene oxide (GO) [22] and some metal oxides such as ZnO [23], and TiO_2 [24], have been co-deposited in Ni-P coating, inhibiting the growth of bacteria on the coating surface. These have been deposited on substrates such as stainless steel and carbon steel, but none of them has been evaluated on polymer substrates such as ABS, nor on parts manufactured by additive manufacturing. In addition, some of the proposed methods use techniques of complex scalability. E. Fayyad et al. [25], co-deposited TiNi metal nanoparticles into Ni-P coating matrix. For this purpose, they added different proportions of nanoparticles (0.2, 0.4 and 0.8 g/L) to an electroless bath, successfully generating nanostructured coatings on APIX100 carbon steel substrates. The authors evidenced that coatings with 0.8 g/L nanoparticle concentration reduced cell viability of *S. aureus* by 70% in respect to a coating without nanoparticles. Also, Z. Sharifalhoseini [26], implemented a sono-synthesis method with which he simultaneously synthesized and deposited zinc oxide nanotubes on Ni-P coatings. Results showed that the percentage inhibition of *E. coli* bacterial growth for Ni-P and Ni-P coated plates with zinc oxide nanoparticles was around 30% and 95%, respectively, compared to the substrate without any coating.

Meanwhile, conventional methods for the generation of coatings on the ABS surface begin with an etching process, which seeks to generate porosity on the surface through the use of chromic and sulfuric acid solutions. Then, the pieces are subjected to an activation stage in different functions that involve palladium or silver, seeking to generate catalytic sites in which to generate the deposition of metals. Finally, the piece is subjected to an electroless coating stage [4]. Etching processes involve compounds with hexavalent chromium ions, which are highly restricted and represent serious environmental risks due to their toxic and carcinogenic nature [27], making it necessary to implement alternative methods that allow the formation of an electroless coating that adheres properly to the surface of the polymeric material. Moreover, the activation processes increase the operation costs due to the components employed [28].

Given the interest in having metallized surfaces with antibacterial properties on substrates obtained by additive manufacturing, this research aims to confer antibacterial properties on electroless Ni-P coatings modified with ZnO nanoparticles, which are deposited on ABS substrates manufactured by fused filament manufacturing (FFF) technology without using chromic acid or palladium during the process. This systematic study provides a novel proposal since no studies generating electrically free Ni-P coatings with antibacterial properties on polymeric substrates have yet been reported. Morphology, chemical composition, kinetics, and antibacterial properties of the coating as a function of concentration of nanoparticles in the electroless bath were studied.

2 Experimental

2.1 Substrate preparation

ABS substrates were manufactured on a Cube 3D printer (Flsun, China) with printing dimensions of 40 × 40 × 60 cm (Equivalent to 96000 cm^3), using fused filament manufacturing (FFF) technology. The printing principle of this technology consists of the extrusion of the material through a nozzle and its subsequent deposition on a hot platform, thus forming a two-dimensional layer on top of another, which results in the desired three-dimensional object [29]. Parts with sizes of 1 × 1 × 0.5 cm and 5 × 5 × 0.5 cm were manufactured; the printing parameters used are specified in Table 1.

2.2 Surface activation

The surface of the printed ABS substrates was mechanically modified using the high-pressure sand ablation technique (sandblasting), with Al_2O_3 alumina (99.0%, Gresco Products, England) with a size of 110 µm at a pressure of 0.10 MPa. These were then chemically etched with a solution of 200 mL/L sulfuric acid (H_2SO_4) (96.0%, Panreac Applichem, Spain) and 240 mL/L hydrogen peroxide (H_2O_2) (33.0%, Panreac Applichem, Spain) for 10 min at 40°C. Both processes were performed with the intention of modifying the surface roughness to increase the adhesion of the subsequent coating to the substrate.

Table 1 Printing parameters used to obtain ABS substrates

Processing parameters	
Infill (%)	20
Infill pattern	Grid
Shells	4
Layer height (mm)	0.15
Extrusion width (mm)	0.4
Printing temperature (°C)	220
Bed temperatura (°C)	60
Print speed (mm/s)	60

The substrates were then rinsed with distilled water and dried completely with a warm air stream. Substrates underwent a sequential surface activation process as follows: hexahydrate nickel sulphate ($NiSO_4$ $6H_2O$) (98.0%, Sigma-Aldrich, USA) at 21.1 g/L and sodium borohydride ($NaBH_4$) (98.0%, Sigma-Aldrich, USA) at 10 g/L were used as the reducing agent. The pieces were immersed in the nickel sulfate solution for 2 min and a stream of warm air was used to promote the adhesion of the salt to the surface (Activation 1). They were then immersed for 10 s in the sodium borohydride (Activation 2) and the process was performed in duplicate (Activation 3 and 4). Finally, the substrates were rinsed with distilled water and dried completely with a warm air stream. The purpose of the activation process is the precipitation of nickel on the surface of the substrate, generating nucleation points that will allow the subsequent formation of the electroless coating on the surface.

2.3 Electroless Ni–P deposition

The surface modified substrates were subjected to a process of electroless Ni-P coating. For this, the substrates were immersed for 30 min, at a temperature of 60°C, in an Ni-P electroless bath supplied by the company SUMICOL S.A.S. The pH of the bath was adjusted to 6.5. Immediately, the substrates were then immersed in a second electroless Ni-P bath in which antibacterial zinc oxide nanoparticles, supplied by the company SUMICOL S.A.S, were incorporated. The formulation of this electroless bath and the process conditions are shown in Table 2.

2.4 Characterization

The physical and chemical characterizations of the substrate surface were initially studied by measuring the contact angle using the Standard Goniometer Ramé - Hart 150W Fiber Optics illuminator (Ramé-hart Instrument Co., USA). The chemical composition was studied using Fourier transform infrared spectroscopy (FTIR – ATR), in the Spectrometer Spectrum Two - PerkinElmer u ATR TWO (PerkinElmer, USA).

The ZnO nanoparticles were characterized by X-ray diffraction (XRD) using a Panalytical Aeris device (Malvern Panalytical, UK) with the θ = 2θ (Bragg Brentano) configuration equipped with monochromatic Cu Kα radiation (λ = 0.154 nm), with a step size of 0.0217 ° and step interval of 0.3 s. Additionally, the particle size and morphology were studied by electron transmission microscopy (TEM) using a Tecnai G2 F20 device (FEI Company, USA).

Table 2. Chemical composition and operating conditions of electroless Ni-P bath with nanoparticles of ZnO

Component	g/L	Purity (%)	Manufacturer/Country of origin
Nickel sulfate	25.0	98.0	Fabroquim/Colombia
Sodium hypophosphite	20.0	99.0	Panreac Applichem/Spain
Sodium citrate	20.0	99.0	Panreac Applichem/Spain
SDS	0.1	98.0	Sigma Aldrich/USA
ZnO Nanoparticles	0.5–1.0–2.0	90.0	Sumicol S.A.S./Colombia
Operating conditions			
Temperature (°C)	60		
pH	10.5		
Time (min)	2.5–5.0–7.5		

The morphological and microchemical examinations of the electroless Ni-P coatings were carried out using a JEOL JSM 6490LV electron scanning microscope equipped with an X-ray dispersive energy spectroscope OXFORD INCAPentaFET-x3 (SEMTech Solutions, USA). These examinations on the electroless Ni-P with ZnO nanoparticles coatings were carried out using a Phenom X desktop SEM/EDS (Thermo Fisher Scientific, USA). The coatings formed were analyzed from a top view and a cross-sectional view. For preparation of the cross section, the probe was cut perpendicular to the growth of the coating and then embedded in acrylic resin, before being polished to a mirror shine using 80 to 2500 grade sandpaper and finally with a damp polishing cloth.

The adhesion of electroless Ni–P on ABS was evaluated under the standard ASTM D 3359. For this, pieces with dimensions of 5.0 × 2.5 × 0.5 cm were manufactured, and the adhesion was evaluated qualitatively on a scale of 0 to 5. To verify the presence of the zinc oxide nanoparticles within the electroless Ni-P layer, X-ray photoelectron spectroscopy (XPS) was performed using an X-ray photoelectronic spectrometer (NAP-XPS) Specs with a PHOIBOS 150 1D-DLD analyzer (Specs GmbH, Germany), using a monochromatic source of Al-Kα (1486.7 eV, 13 kV, 100 W) with pass-through energy of 85.36 eV for general spectra and 20 eV for high resolution spectra. General spectra were determined at 1.0 eV, as well as 0.1 eV for high-resolution spectra. Finally, the kinetics of the Ni-P with zinc oxide nanoparticles coating was studied as a function of the concentration of nanoparticles in the electroless bath and the coating time.

2.5 Antibacterial activity test

The antibacterial behavior of Ni-P coatings with zinc oxide nanoparticles at different concentrations of nanoparticles was evaluated under JIS Z 2801 standard. Antibacterial activity was determined by counting colony-forming units for *Staphylococcus aureus* ATCC 6538 over 24 h of inoculation. In addition to the plate containing ZnO, another plate without ZnO was tested with the aim of excluding the effect of the Ni-P coating on the antibacterial activity.

3 Results and discussion

3.1 Surface modification characterization

Figure 1 shows the interaction between a water drop and substrate at each surface modification stage. It is evidenced that the substrates of printed ABS show a typical hydrophilic behavior (Fig. 1a), which is modified by mechanical treatment through sandblasting, leading to a hydrophobic character which is preserved after the etching stage or chemical treatment (Fig. 1b and c). This corresponds to what is expected since, during this treatment, microporosity is generated on the surface of the substrate, increasing its specific surface area, and therefore increasing the interaction with the drop of water, with the sandblasting process having the same effect. Finally, during the activation stages Fig. 1(d)–(g) in which nickel precipitation is generated on the surface of the substrate, the hydrophilic character is returned to the substrate and active anchoring points are generated for the growth of the electroless coating.

Figure 2 shows the FTIR spectrum of the substrate during surface modification processes. Initially, it is possible to evidence the characteristic peaks of ABS as follows: =CH by the movement of the aromatic ring in styrene at 3083, 3061, 3027 and 3004 cm^{-1} (n stretching) and 965 cm^{-1} by trans butadiene (δ bending), 873, 728 and 699 cm^{-1} derivatives to the aromatic ring (δ bending); $=CH_2$ by vibrations associated with butadiene at 2922, 2851, 1453 and 759 cm^{-1} (n_{as}, n_s stretching/δ_s, δ_ω bending respectively); C≡N due to acrylonitrile at 2237 cm^{-1} (n_s stretching); -C-O to 1261 cm^{-1}, 1246 cm^{-1}, 1118 cm^{-1}, 1098 cm^{-1} (n stretching) and -C=O to 1718 cm^{-1} (n stretching) due to, possibly, the presence of carbonyl groups attributed to an ester group, which is typically found in additives added to the ABS, and used as a heat stabilizer belonging to the class of sterically hindered

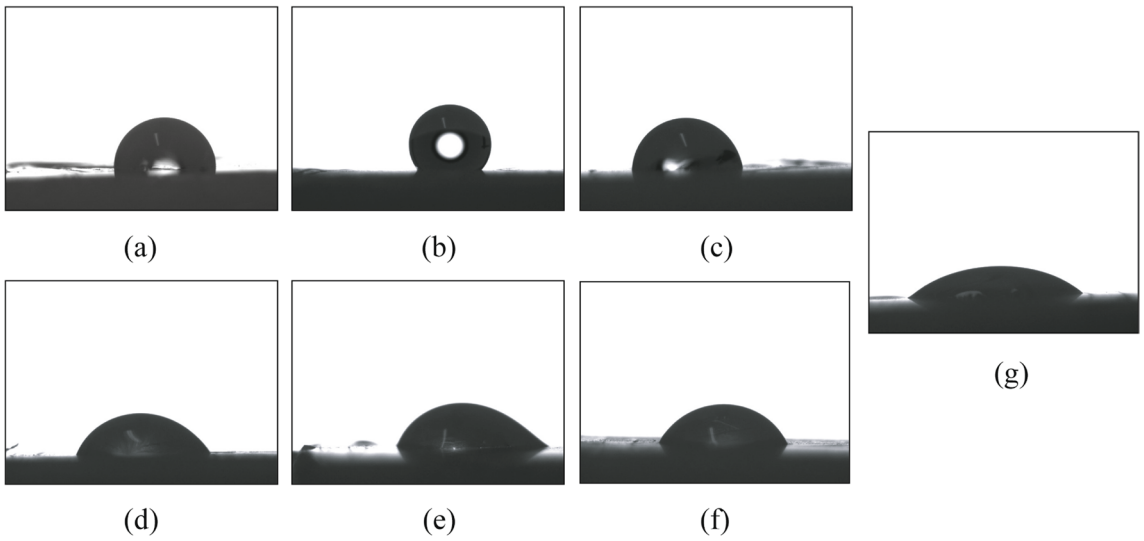

Fig. 1 Determination of contact angle during surface modification of ABS substrates, **a** ABS substrate, **b** sandblasted, **c** etched, **d** activated 1, **e** activated 2, **f** activated 3, **g** activated 4

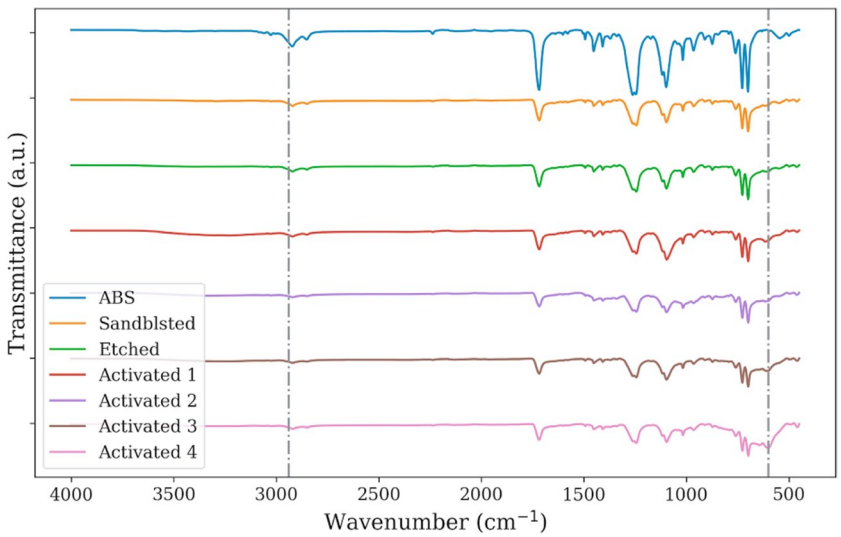

Fig. 2 FTIR spectra of the substrate during the surface modification process of ABS substrates

phenolic antioxidants [30]. These peaks are retained throughout the process but are slightly attenuated during surface modification of the substrate. Subsequently, during the activation stages, the presence of a peak at 610 cm^{-1} corresponding to the Ni-O (n stretching) content becomes evident [30]. This corresponds to the increase in catalytic points on the surface of the substrate, which are consistent with the results obtained in the measurements of contact angles.

Based on both analyses, it is possible to determine that the change in wettability evidenced in Fig. 1(a, b, c) is related to the generation of pores due to the applied etching methodologies, which modify the physical interaction of the substrate with water, and not by the generation of chemical modifications in the composition of the substrate.

3.2 Electroless Ni–P coating on ABS characterization

Figure 3(a) and (b) shows the morphological characterization of the Ni-P coating deposited after the activation process for 30 min of immersion in the electroless bath. The formation of a compact structure is observed, without the presence of cracks or pores on its surface, and with a cauliflower-type morphology that is characteristic of the Ni-P growth. Regarding the cross-section of the coating, Fig. 3(c)

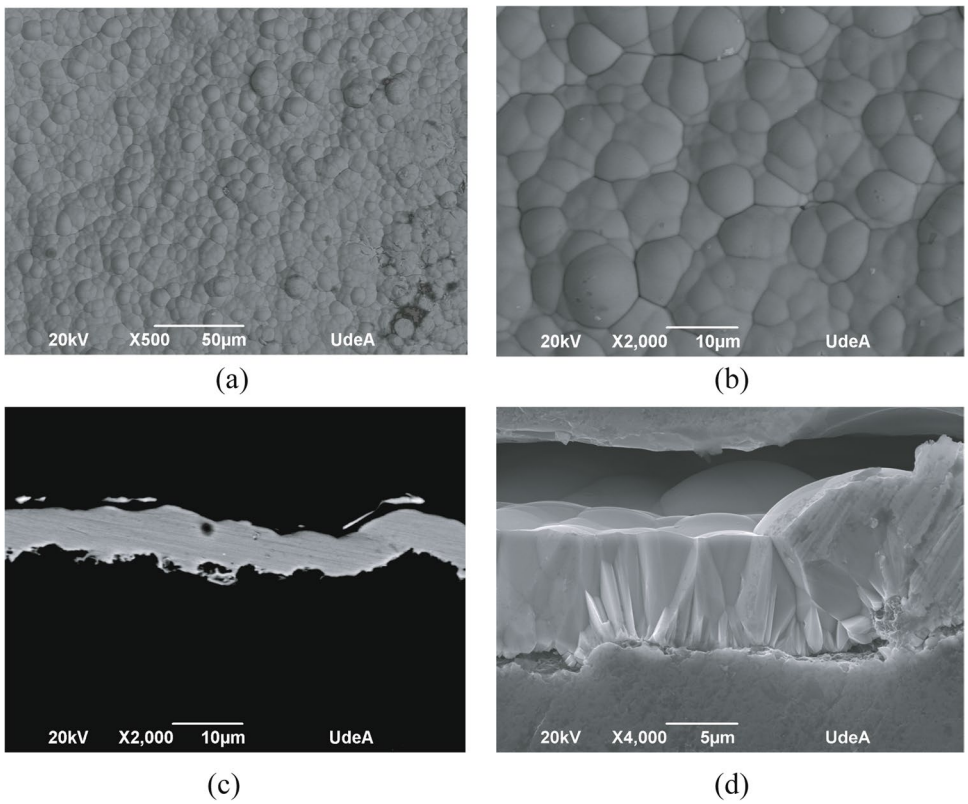

Fig. 3 SEM images of electroless coating Ni-P on ABS. **a** and (**b**) top view, **c** and (**d**) cross-section

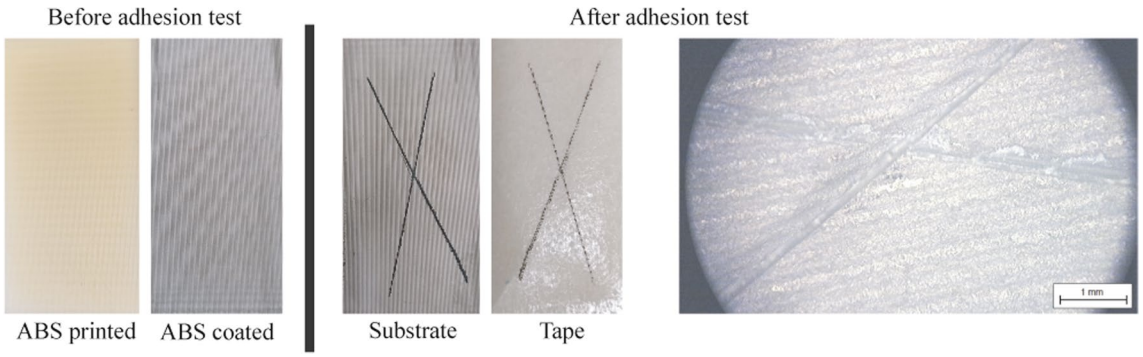

Fig. 4 Optical microscope images of adhesion tests of electroless Ni-P coatings formed on ABS substrates

and (d) shows that there was a continuous deposition of the coating, without dislocations or defects, and a columnar growth, typical in this type of coating. Figure 4 shows the adhesion test carried out under the ASTM D 3359 standard to analyze the adhesion of the substrate. With this, it is possible to classify the adhesion of the coating with the substrate in 5A, showing that the etching, activation and coating methodologies implemented are satisfactory.

Based on both analyses, it is possible to show that, from the proposed etching methodology, porosity is generated on the surface that allows the anchoring of the coating. An example of the above is shown in Fig. 3(c), in which the generation of the coating is observed along the entire surface of the substrate. This also allows the initiation of the autocatalytic reaction of electroless deposition process due to the generation of catalytic sites correctly distributed on the surface. The implementation of the proposed surface modification steps allows the adhesion of the coating on the substrate and their growth, satisfying the typical characteristics of Ni-P electroless coatings such as their morphology.

3.3 Nanoparticles characterization

Figure 5(a) shows a TEM image of the zinc oxide nanoparticles that were used for the formation of the antibacterial coating. The nanomaterial exhibits a quasi-prismatic

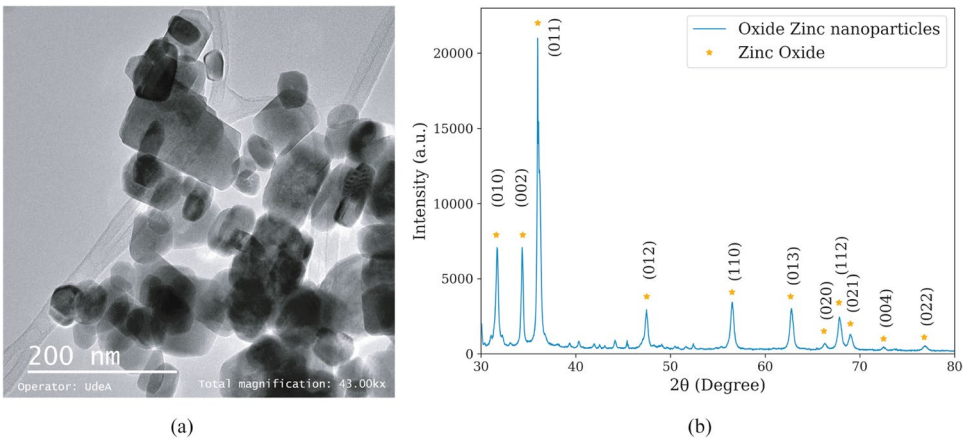

Fig. 5 (**a**) TEM image and (**b**) XRD analysis of zinc oxide nanoparticles

morphology with dispersion in its particle size between 30 and 90 nm. On the other hand, Fig. 5(b) shows the X-ray diffraction patterns of the ZnO nanoparticles. The diffractogram shows peaks which are attributed to the planes including (010), (002), (011), (012), (110), (013), (020), (112), (021), (004) and (202). The pattern matched well with the standard JCPDS Data Card No. 89-1397. The peaks identified around 40° and 50° correspond to contaminations of anhydrous zinc acetate coming from residues of the synthesis precursors [27].

3.4 Electroless Ni–P–ZnO nanoparticles characterization

Figure 6(a) shows the morphology obtained by SEM microscopy of electroless Ni-P coatings with zinc oxide nanoparticles, formed at different deposition times and different concentration of nanoparticles in the electroless bath. In all cases, it is possible to observe typical cauliflower morphologies. There is no evidence of a considerable change in the morphology of the coating due to the content of nanoparticles.

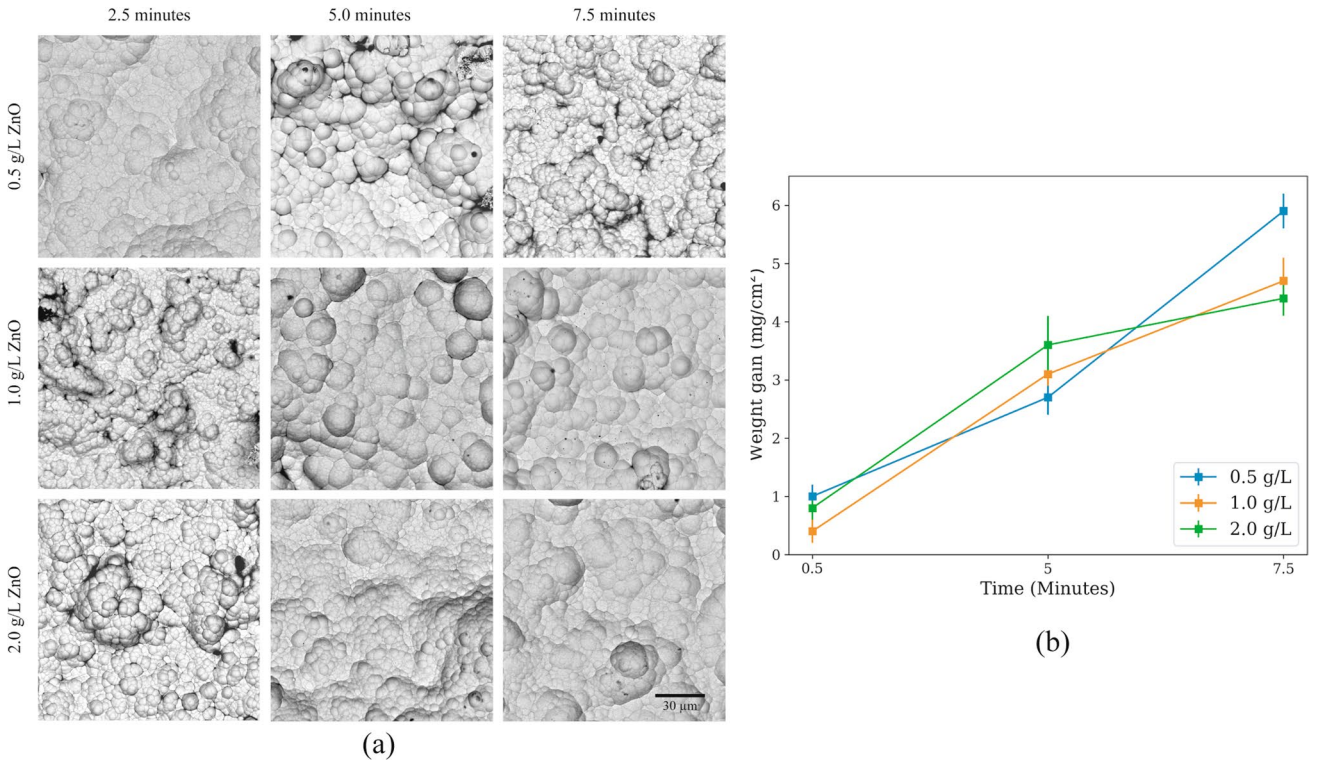

Fig. 6 (**a**) SEM images of Ni-P electroless coatings with co-deposited ZnO nanoparticles at different concentrations and (**b**) weight change of Ni-P electroless coatings with zinc oxide nanoparticles as a function of deposition time and concentration of nanoparticles in the electroless bath

Additionally, as the deposition time increases, greater compaction and homogeneity of the structures are evidenced. This is consistent with the deposition kinetics of electroless Ni-P coatings, where longer coating formation times promote the growth of already deposited grains that are coated by the Ni-P alloy [31]. On the other hand, when analyzing the formation kinetics of the coating shown in Fig. 6(b), a clear trend of proportional growth in the gain in weight of the coating is observed as the deposition time increases, a situation that is in agreement with the self-catalytic nature of the coating [32]. However, there is no significant correlation between the gain in weight of the coating and the content of nanoparticles in the electroless bath. Therefore, this is not a relevant factor in the deposition kinetics of the coating. The catalytic deposition kinetics of the electroless Ni-P predominate in the weight gain of the coating [33].

Figure 7(a) shows the Zn content in the coatings versus deposition time at different concentrations of these in the electroless bath. It is observed that the higher the concentration of nanoparticles, the greater the Zn content on the surface. This is in accordance with expectations since, while some of these nanoparticles are coated (especially in early stages of growth) by the Ni-P alloy [30], another part is a secondary phase that ascends to the surface with the growth of the coating, such that the higher the number of nanoparticles incorporated, the greater the amount of zinc finally observed. In accordance with the above, the lower deposition times show a higher percentage of zinc because much of the nanoparticles have not been coated until then, a situation that changes over time, as seen in Fig. 7(a). Based on the above and considering the dependence between weight and deposition time described above, a 5-min deposition time appears to be sufficient to ensure adequate morphology and quantity of nanoparticles of ZnO on the surface. To analyze the state of the nanoparticles in the coating, Fig. 7(b) shows the cross section of one of the deposited coatings, showing homogeneity in the deposited coating, good adhesion between the Ni-P coating and the Ni-P-ZnO coating, and no evidence of nanoparticle clusters. Furthermore, Fig. 7(c) and (d) shows high-resolution XPS spectra of Ni-P electroless coatings with nanoparticles of ZnO. The core level spectrum of Zn 2p is shown in

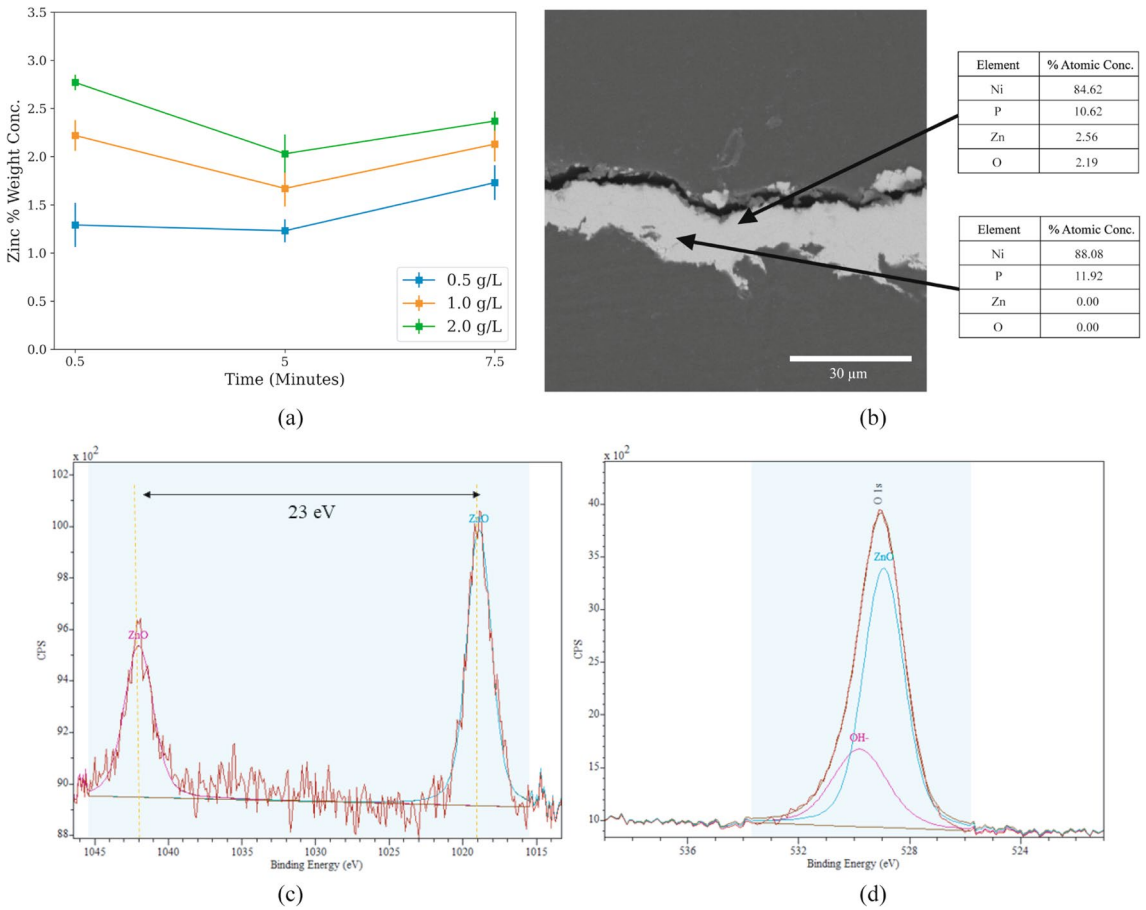

Fig. 7 (**a**) Zinc content at different deposition times, (**b**) SEM/EDS image, (**c**) Zn 2p XPS spectra and (**d**) O1s XPS spectra of electroless Ni-P coatings with zinc oxide nanoparticles

Fig. 7(c). In this, it is possible to observe the characteristic double of Zn 2p, where the peaks associated to zinc oxides in 1018 eV for Zn 2p2/3 and 1041 eV for Zn 2p1/2 are clearly present; with a separation between both peaks equal to 23 eV [31]. Similarly, the spectrum for oxygen O 1s is shown in Fig. 7(d). Here, the peak at 528.8 eV associated with O^{2-}, which is also associated with metal bonds, in this case Zn, is observed, and another peak at 529.8 eV associated with bonds between hydroxyl groups, coming from the nanoparticle synthesis process. In this way, it can be ensured that, through the proposed coating methodology, co-deposition of zinc oxide nanoparticles together with the Ni-P electroless coating is possible.

Based on the results obtained, Fig. 8 shows a graphical representation of the entire process, including the 3D printing process of the substrates, and each of the stages of surface modification, activation and electroless Ni-P coatings.

3.5 Antibacterial characterization

Figure 9 shows a decrease in the colony-forming units of the bacterium *S. aureus* in the Ni-P electroless coatings with zinc oxide nanoparticles compared to the coating without nanoparticles. The above indicates a modification of the antibacterial behavior of the surface such that, thanks to the presence of nanoparticles, it is possible

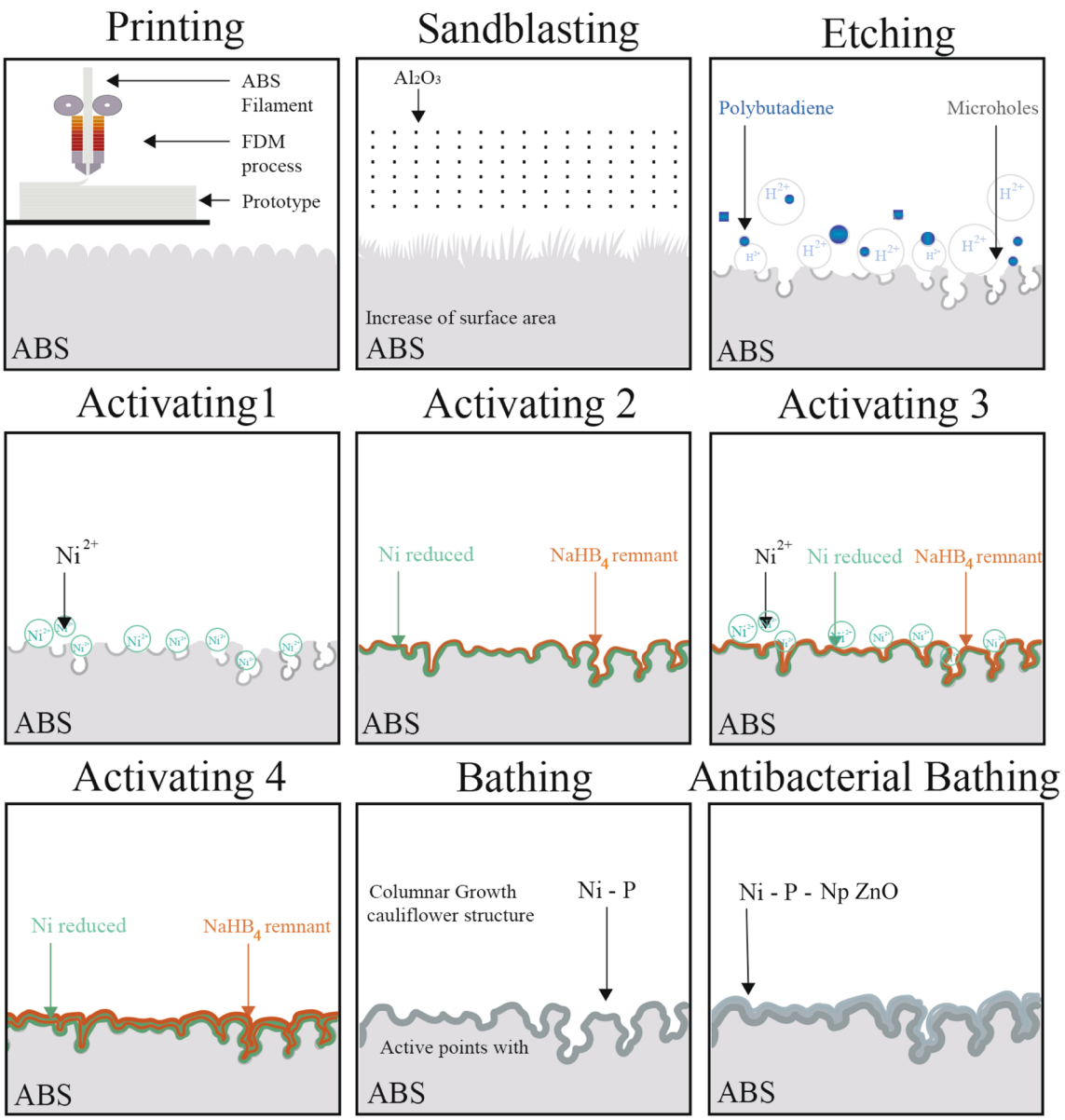

Fig. 8 Schematic process of electroless coating Ni-P with nanoparticles of ZnO on ABS substrates produced by additive manufacturing

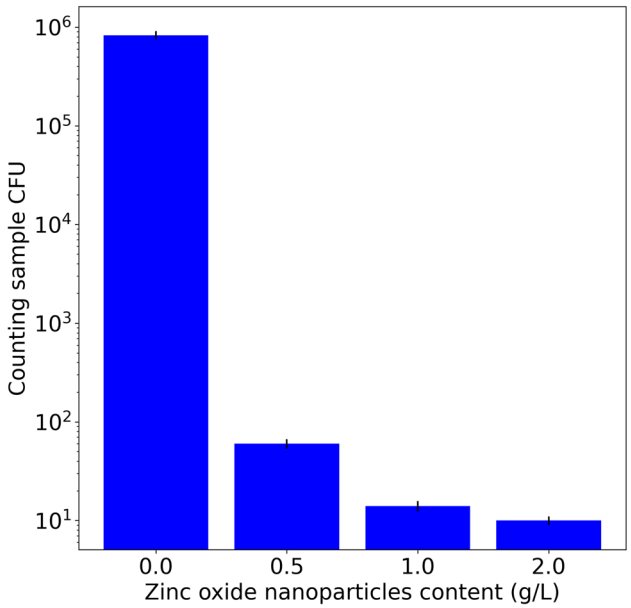

Fig. 9 Antibacterial behavior of electroless Ni-P coatings with 0, 0.5, 1.0 and 2.0 g/l of ZnO nanoparticles

to interact with bacteria by inhibiting their growth and preventing their propagation [34]. In addition, considering that antibacterial behavior was evaluated for samples with a deposition time of 5 min (which is corroborated as sufficient to guarantee the behavior), the increase in the content of nanoparticles in the coating (0.5, 1.0 and 2.0 g/L) generates a decrease of 75, 92 and 95% in colony-forming units and an increase in antibacterial activity on the surface.

Table 3 summarizes the main characteristics obtained in the proposed methodology based on the results obtained. Based on the results obtained, the developed coatings have a potential use in industries such as bathrooms and kitchens, automotive accessories, and others, due to the addition of ZnO nanoparticles that confer antibacterial properties to the parts, modifying their surface characteristics and promoting their use in other environments.

4 Conclusions

Electroless Ni-P coatings with zinc oxide nanoparticles were successfully deposited on 3D printed ABS substrate, implementing chromium-free and palladium-free methodologies. The Ni-P coating deposited on the polymer surface of the ABS exhibits a good relationship in its substrate-coating interface and a compact formation, with a cauliflower type morphology typical of these coatings. In addition, it is possible to observe changes in the surface characteristics of the substrate at each stage of surface modification.

Co-deposition of zinc oxide nanoparticles in the electroless Ni-P coating allows modification of the antibacterial properties of the coating, and there is a directly proportional relationship between the concentration of nanoparticles and the antibacterial activity of the surface. This is reflected in the correspondence between the concentration of nanoparticles (0.5, 1 and 2 g/L) and the amount of Zn observed on the surface of the coating, for all times studied (0.5, 5 and 7.5 min). In addition, it was observed that the number of nanoparticles in the bath affects the morphology of the coatings, such that the higher the concentration, the greater the number of nucleation points, which generates a refinement in the grain size. However, these same variables do not significantly affect the deposition kinetics of the electroless bath, the deposition time being the variable of greatest influence in this aspect. This work demonstrates that it is possible to form antibacterial surfaces by co-depositing electroless Ni-P coatings and ZnO nanoparticles on ABS surfaces fabricated through 3D printing. This opens up the possibility of using these parts in environments that are prone to bacterial propagation, thereby expanding their range of applications. Furthermore, evidence indicates that it is possible to create coatings on ABS using processes that are chromium- and palladium-free.

Table 3 Summary of main characteristics of electroless Ni-P and Ni-P composite coatings

Characteristic	Electroless Ni-P	Electroless Ni–P with ZnO nanoparticles		
		0.5 g/L	1 g/L	2 g/L
Adherence (D 3359)	5 A	-	-	-
Weight gain (mg/cm^2)*	-	2.7 ± 0.3	3.1 ± 0.2	2.6 ± 0.5
Identified nanoparticles content (%Weight Conc.)*	-	1.23 ± 0.12	1.67 ± 0.19	2.03 ± 0.2
Antibacterial behavior - JIS Z 2801 (Counting sample CFU)	$8.3 \times 10^5 \pm 0.8 \times 10^5$	$6.0 \times 10^1 \pm 0.7 \times 10^1$	$1.4 \times 10^1 \pm 0.2 \times 10^1$	$1.0 \times 10^1 \pm 0.1 \times 10^1$

*5 min of deposition

Author contribution S. Restrepo: investigation, formal analysis, writing—original draft and visualization; M.P. Duque: investigation, writing—original draft and visualization; S. Bello: investigation, writing—original draft and visualization; L.M. Tirado: investigation; F. Echeverría: conceptualization, formal analysis, methodology and funding acquisition; A.A Zuleta: conceptualization, formal analysis, data curation, funding acquisition and writing—review & editing; J.G. Castaño: conceptualization, formal analysis, methodology and writing—review & editing; E. Correa: conceptualization, formal analysis, methodology, data curation and funding acquisition and writing—review & editing

Funding Open Access funding provided by Colombia Consortium The authors are grateful for the funding received from the Universidad de Medellín, Centro de Investigación para el Desarrollo y la Innovación (CIDI) from the Universidad Pontificia Bolivariana (Rad:635C-11/20-35), Universidad de Antioquia, Corporación Ruta N and Sumicol S.A.S. within the framework of "Convocatoria conjunta de proyectos de I+D+i en el marco de la agenda regional de I+D → i año 2020" funded by the Universidad Pontificia Bolivariana, Universidad Nacional de Colombia sede Medellín, Universidad EIA, Universidad EAFIT, Universidad de Medellín, Universidad de Antioquia, Universidad CES, Institución Universitaria ITM and Corporación Universitaria Lasallista.

Declarations

Conflict of interest The authors declare no competing interests.

References

1. Jia Y, Chen J, Asahara H et al (2020) Photooxidation of the ABS resin surface for electroless metal plating. Polymer 200:122592. https://doi.org/10.1016/j.polymer.2020.122592
2. Pérez Fernández M (2018) Nueva generación de materiales plásticos basados en ABS de altas prestaciones técnicas o más sostenibles con el medio ambiente. Universidad Autónoma de Barcelona. Barcelona. http://hdl.handle.net/10803/664173
3. Blyweert P, Nicolas V, Fierro V, Celzard A (2021) 3D printing of carbon-based materials: a review. Carbon N Y 183:449–485. https://doi.org/10.1016/j.carbon.2021.07.036
4. Bazzaoui M, Martins JI, Bazzaoui EA et al (2013) A simple method for acrylonitrile butadiene styrene metallization. Surf Coat Technol 224:71–76. https://doi.org/10.1016/j.surfcoat.2013.02.050
5. Jones KE, Patel NG, Levy MA et al (2008) Global trends in emerging infectious diseases. Nature 451:990–993. https://doi.org/10.1038/nature06536
6. Cloutier M, Mantovani D, Rosei F (2015) Antibacterial coatings: challenges, perspectives, and opportunities. Trends Biotechnol 33:637–652. https://doi.org/10.1016/j.tibtech.2015.09.002
7. Ogunsona EO, Muthuraj R, Ojogbo E et al (2020) Engineered nanomaterials for antimicrobial applications: a review. Appl Mater Today 18:100473. https://doi.org/10.1016/j.apmt.2019.100473
8. Vu TV, Nguyen VT, Nguyen-Tri P et al (2020) Antibacterial nanocomposite coatings. In: Nanotoxicity. Elsevier, pp 355–364
9. Sahoo P, Das SK (2011) Tribology of electroless nickel coatings - a review. Mater Des 32:1760–1775. https://doi.org/10.1016/j.matdes.2010.11.013
10. Sudagar J, Lian J, Sha W (2013) Electroless nickel, alloy, composite and nano coatings - a critical review. J Alloys Compd 571:183–204. https://doi.org/10.1016/j.jallcom.2013.03.107
11. Algul H, Uysal M, Alp A (2021) A comparative study on morphological, mechanical and tribological properties of electroless NiP, NiB and NiBP coatings. Appl Surf Sci 4:100089. https://doi.org/10.1016/j.apsadv.2021.100089
12. Zhang B (2016) Nano electroless plating. In: Amorphous and nano alloys electroless depositions, Chemical I, Elsevier, pp. 141–289. https://doi.org/10.1016/B978-0-12-802685-4.00004-2
13. Tamilarasan TR, Rajendran R, Siva Shankar M et al (2016) Wear and scratch behaviour of electroless Ni-P-nano-TiO2: effect of surfactants. Wear 346–347:148–157. https://doi.org/10.1016/j.wear.2015.11.015
14. Dong D, Chen XH, Xiao WT et al (2009) Preparation and properties of electroless Ni-P-SiO2 composite coatings. Appl Surf Sci 255:7051–7055. https://doi.org/10.1016/j.apsusc.2009.03.039
15. Zhou G, Ding H, Zhou F, Zhang Y (2008) Structure and mechanical properties of Ni-P-nano Al2 O3 composite coatings synthesized by electroless plating. J Iron Steel Res Int 15:65–69. https://doi.org/10.1016/S1006-706X(08)60014-X
16. Zhang S, Han K, Cheng L (2008) The effect of SiC particles added in electroless Ni-P plating solution on the properties of composite coatings. Surf Coat Technol 202:2807–2812. https://doi.org/10.1016/j.surfcoat.2007.10.015
17. Galvis O, Zuleta A, Torres H et al (2007) Obtención y evaluación de recubrimientos Ni-P modificados con magnetitas sintetizadas en presencia de y Ce. Scientia et Technica 36:387–391. https://doi.org/10.22517/23447214.5087
18. Balaraju JN, Sankara Narayan TSN, Seshadri SK (2003) Electroless Ni-P composite coatings. J Appl Electrochem 33:807–816
19. Li J, Ma Q, Shao H et al (2017) Biosynthesis, characterization, and antibacterial activity of silver nanoparticles produced from rice straw biomass. Bioresources 12:4897–4911. https://doi.org/10.15376/biores.12.3.4897-4911
20. Sirelkhatim A, Mahmud S, Seeni A et al (2015) Review on zinc oxide nanoparticles: antibacterial activity and toxicity mechanism. Nano Lett 7:219–242. https://doi.org/10.1007/s40820-015-0040-x
21. Slavin YN, Asnis J, Häfeli UO, Bach H (2017) Metal nanoparticles: understanding the mechanisms behind antibacterial activity. J Nanobiotechnology 15:1–20. https://doi.org/10.1186/s12951-017-0308-z
22. Shao W, Wu J, Liu H et al (2016) Graphene oxide reinforced Ni-P coatings for bacterial adhesion inhibition. RSC Adv 6:46270–46277. https://doi.org/10.1039/c6ra04408e
23. Sharifalhoseini Z, Entezari MH, Jalal R (2015) Evaluation of antibacterial activity of anticorrosive electroless Ni-P coating against Escherichia coli and its enhancement by deposition of sono-synthesized ZnO nanoparticles. Surf Coat Technol 266:160–166. https://doi.org/10.1016/j.surfcoat.2015.02.035
24. Zhao Q, Liu C, Su X et al (2013) Antibacterial characteristics of electroless plating Ni – P – TiO 2 coatings. Appl Surf Sci 274:101–104. https://doi.org/10.1016/j.apsusc.2013.02.112

25. Fayyad EM, Hassan MK, Rasool K et al (2019) Surface & Coatings Technology Novel electroless deposited corrosion — resistant and anti-bacterial NiP – TiNi nanocomposite coatings. Surf Coat Technol 369:323–333. https://doi.org/10.1016/j.surfcoat.2019.04.064
26. Sharifalhoseini Z, Entezari MH (2015) Enhancement of the corrosion protection of electroless Ni–P coating by deposition of sonosynthesized ZnO nanoparticles. Appl Surf Sci 351:1060–1068. https://doi.org/10.1016/j.apsusc.2015.06.028
27. Moezzi A, Cortie MB, McDonagh AM (2013) Zinc hydroxide sulphate and its transformation to crystalline zinc oxide. Dalton Trans 42:14432–14437. https://doi.org/10.1039/c3dt51638e
28. Suman R, Nandan D, Haleem A et al (2020) Experimental study of electroless plating on acrylonitrile butadiene styrene polymer for obtaining new eco-friendly chromium-free processes. Mater Today: Proc 28:1575–1579. https://doi.org/10.1016/j.matpr.2020.04.843
29. Dizon JRC, Espera AH, Chen Q, Advincula RC (2018) Mechanical characterization of 3D-printed polymers. Addit Manuf 20:44–67. https://doi.org/10.1016/j.addma.2017.12.002
30. Krishnamurti D (1958) The Raman spectra of crystalline sulphates of Ni and Mn. Proc Indian Acad Sci 48:355–363. https://doi.org/10.1007/BF03052920
31. Zuleta AA, Correa E, Castaño JG et al (2017) Study of the formation of alkaline electroless Ni-P coating on magnesium and AZ31B magnesium alloy. Surf Coat Technol 321:309–320. https://doi.org/10.1016/j.surfcoat.2017.04.059
32. Momenzadeh M, Sanjabi S (2012) The effect of TiO 2 nanoparticle codeposition on microstructure and corrosion resistance of electroless Ni-P coating. Materials and Corrosion 63:614–619. https://doi.org/10.1002/maco.201005985
33. Kumar K, Bansal V, Sharma S et al (2022) Microhardness and wear resistance of alkaline electroless Ni-P/Ni-P-ZnO nanocomposite platings. Mater Today Proc. https://doi.org/10.1016/j.matpr.2022.12.213
34. Emami-Karvani Z (2012) Antibacterial activity of ZnO nanoparticle on Gram-positive and Gram-negative bacteria. Afr J Microbiol Res 5:1368–1373. https://doi.org/10.5897/ajmr10.159